Carbohydrate Polymer Technologies and Applications 2 (2021) 100047

Contents lists available at ScienceDirect

Carbohydrate Polymer Technologies and Applications

journal homepage: www.elsevier.com/locate/carpta

Concentrated regimes of xanthan-based hydrogels crosslinked with multifunctional crosslinkers

Ghazaleh Azizi Saadatlou[1], Gholamreza Pircheraghi*

Polymeric Materials Research Group (PMRG), Materials Science and Engineering Department, Sharif University of Technology, Tehran, Iran

ARTICLE INFO

Keywords:
Xanthan hydrogel
Multifunctional crosslinker
Rheological behavior
FTIR
POM
SEM

ABSTRACT

Samples were synthesized via solution mixing method with a concentration of 4wt.% of Xanthan and 0, 1, 2 or, 3 wt.% of bi-functional and tetra-functional crosslinkers, i.e. citric acid and Borax, respectively. The rheological studies at two different temperatures showed an unanticipated increase in the storage modulus values with increasing temperature which is due to the conformational change from ordered helix to disordered coils in Xanthan molecules. Thus, it is hypothesized that the concentration of Xanthan and the crosslinking density in the system play crucial roles in the conformational change of the molecules. Polarized optical microscopy (POM), FTIR, and SEM results showed that in the crosslinked samples conformational change is prevented stronger than the native sample. POM images revealed that higher crosslinking density in Xanthan – Borax hydrogels causes bigger regions of crystalline phase compared to Xanthan – citric acid hydrogels, pointing at the effect of the tetra-functional crosslinking agent. Also, SEM imaging showed that higher crosslinks density has led to smaller pore sizes in the freeze-dried samples. FTIR analysis proved that the stronger effect of Borax is due to higher crosslinking density in Xanthan-Borax samples. Finally, a mechanism for crosslinking of Xanthan with Borax was suggested.

1. Introduction

Xanthan gum, a faint yellow powder, is a naturally occurring, water-soluble polysaccharide produced predominantly by Xanthomonas Campestris in aerobic conditions (García-Ochoa, Santos, Casas, & Gómez, 2000). The monomer of the anionic heteropolysaccharide consists of glucose, mannose, and glucuronic acid units with a molecular ratio of 2:2:1 (García-Ochoa et al., 2000). Trisaccharide side chains attached to alternate glucose units by $\alpha - 1,3$ linkages on C-3 positions are composed of a D-glucuronic acid ($\beta - 1,2$) located between two D-mannose units ($\beta - 1,4$). The backbone length of a unit cell has been reported as 0.94 nm (Hamcerencu, Popa, Riess, & Desbrieres, 2019). The molecular weight of Xanthan gum has been reported between $4 - 12 \times 10^3$ KDa in the literature (Michel Milas & Rinaudo, 1979); an accurate amount for molecular weight cannot be measured due to very high molecular weight, the stiffness of the molecule and, the presence of aggregates (Michel Milas & Rinaudo, 1979; Milas, 1990).

Hydrogels are water-swollen crosslinked polymeric three-dimensional networks that form via covalent/non-covalent crosslinks (Ahmed, 2015; Dixit, Bag, Sharma, & Eswara Prasad, 2019). Due to high amounts of absorbed water, hydrogels show a flexibility degree similar to biological tissues, a characteristic that enhances the use of hydrogels in biomedical applications (Kopeček & Yang, 2007; Annabi et al., 2014). Xanthan-based hydrogels are being increasingly reviewed in the literature. The biocompatibility and biodegradability of Xanthan alongside hydrogels' similarity to biological systems, make Xanthan hydrogels interesting materials for biomedical applications (Caló & Khutoryanskiy, 2015). The rheological behavior and microstructure of release-controlled hydrogels based on xanthan gum crosslinked with sodium trimetaphosphate have been reported by (Tao et al., 2016).

Different chemicals such as citric acid (Bueno, Bentini, Catalani, & Petri, 2013), epichlorohydrin (Alupei, Popa, Hamcerencu, & Abadie, 2002b), and sodium trimetaphosphate (STMP) (Tao et al., 2016) have been used as crosslinking agents in Xanthan hydrogels. (Bueno et al., 2013) indicated that Xanthan crosslinking occurs due to esterification reaction in the presence of citric acid. Ester linkages formation also occurs in the absence of acetic acid, between Xanthan acid groups and hydroxyl groups while heating. They showed that these crosslinks affect swelling behavior, pH stability, and hydrogel porosity(Bueno et al., 2013). Superabsorbent hydrogels based on Xanthan and poly(vinyl alcohol) and crosslinked with epichlorohydrin were investigated by (Alupei, Popa, Hamcerencu, & Abadie, 2002a). They showed that the capacity of water uptake and the maximum swelling degree varies with mixture composition, crosslinking time and temperature, and the

* Corresponding author.
E-mail addresses: ghazalehazizi93@student.sharif.edu, gsaadatlou19@ku.edu.tr (G.A. Saadatlou), pircheraghi@sharif.ir (G. Pircheraghi).
[1] Present Address: Materials Science and Engineering Department, Koc University, Istanbul, Turkey.

https://doi.org/10.1016/j.carpta.2021.100047
Received 3 September 2020; Received in revised form 11 February 2021; Accepted 11 February 2021
Available online 14 February 2021
2666-8939/© 2021 The Authors. Published by Elsevier Ltd. This is an open access article under the CC BY-NC-ND license (http://creativecommons.org/licenses/by-nc-nd/4.0/)

crosslinking agent concentration. (Edens, 2005; Sereno, Hill, & Mitchell, 2007) discussed that Xanthan molecules have two conformations: disordered or coil-shaped conformation under low ionic strength or high temperatures, and ordered or helix conformation under low temperatures or high ionic strength. The conformational changes reflect in rheological properties measured in different temperatures and concentrations (Bejenariu, Popa, Picton, & Le Cerf, 2010)(Morris, 2019).

(Bejenariu et al., 2010) have shown that before crosslinking, the conformation of Xanthan chains is dependent on the acidity of the medium; in acidic media, Xanthan chains are always in double helix conformation while in alkaline media they partially transition to coils. In another research, they showed that after crosslinking with sodium trimetaphosphate the presence of crosslinking agent and phosphate ions are oppositely influencing the swelling behavior which can be attributed to the Xanthan chains conformation (Bejenariu, Popa, Dulong, Picton, & Le Cerf, 2009). In 2001, Pelletier et. al., for the first time, used oscillatory shear, steady shear flow, and extensional flow data to investigate the order-disorder transition of Xanthan gum. They concluded that these rheological techniques could be used to track changes in in the molecular scale and the physical network structure (Pelletier, Viebke, Meadows, & Williams, 2001). Most recently, the effect of a surfactant (sodium stearoyl lactylate) on the conformation of κ-carrageenan has been studied by rheometery. It is concluded that the G' and G'' slopes increase with the concentration of the surfactant which is a result of a less organized network in the presence of the surfactant (Ortiz-Tafoya, Rolland-Sabaté, Garnier, Valadez-García, & Tecante, 2018). Brunchi et. al. investigated the changes in characteristics of Xanthan gum chains and intermolecular interactions with changing temperature and ionic strength. These conformational changes were analyzed by ATR-FTIR and then corroborated with viscometry data (Brunchi, Avadanei, Bercea, & Morariu, 2019).

Additionally, it is known that the ordered conformation of Xanthan molecules can form the liquid crystalline (LC) phases which are stable in wide ranges of concentrations (M Milas, Rinaudo, & Tinland, 1985; Iseki, Takahashi, Hattori, Hatakeyama, & Hatakeyama, 2001; Boyd et al., 2009). The formation of the liquid crystalline phase is due to the stable helical structure of the Xanthan molecule arising from the non-covalent bonds, including hydrogen bonding, electrostatic interactions, and the steric hindrance between Xanthan chains as reported in the literature (Li, Rief, Oesterhelt, & Gaub, 1999; Zuev, Kostromin, & Bronnikov, 2008). The polarized optical microscopy (POM) images are used to reveal the LC phase, which forms in Xanthan solutions due to its particular texture (Maret, Milas, & Rinaudo, 1981; Yoshida, Hatakeyama, & Hatakeyama, 1990; Allain, Lecourtier, & Chauveteau, 1988; Dong et al., 2006). In POM imaging, the path lengths of the macromolecule vary with their orientations in the sample, and thus the obtained wavelengths of the transmitted light were changed, producing various colors (Rwei & Nguyen, 2014). Regarding concentrated polysaccharide solutions, it is known that the transition from the liquid crystalline phase to the isotropic phase reduces repulsive interactions and the association between macromolecules depends on the number of hydroxyl groups (Burchard, 2001).

In this study, we aimed to investigate the rheology of 4wt.% Xanthan hydrogels (well above the C^{**} concentration (Cuvelier & Launay, 1986; Oliveira et al., 2013; Southwick, Lee, Jamieson, & Blackwell, 1980; Rodd, Dunstan, & Boger, 2000)) crosslinked using bi-functional (citric acid) and tetra-functional (Borax) crosslinking agents at different temperatures. The main goal is to understand how crosslinking affects the conformational changes by studying the rheological properties and liquid crystalline phase by POM. As discussed earlier, different rheological techniques have been used to study the conformation of the macromolecules and specifically, Xanthan chains. Thus, we have used dynamic shear rheometry and corroborated the resulting data to the probable conformations. According to the literature, 4wt.% Xanthan solution stays in the concentrated regime, in which, the entanglements and conformational changes of the macromolecule play an important role in the rheological behavior of the system. Thus, it has been hypothesized that crosslinking density prevents the conformational change of the Xanthan chains. Also, since Borax is a tetra-functional crosslinking agent, the prevention effect is expected to be stronger than that of citric acid, a bi-functional agent.

2. Experimental

2.1. Materials

Xanthan gum from Xanthomonas Campestris (CAS: 11138-66-2), a faint yellow powder with a 1% solution Brookfield Viscosity of 800 – 1200 cPs and a molecular weight in the range of $4-12\times10^6$ g/mol, citric acid (powder, CAS: 77-92-9), and Borax (powder, CAS: 1330-43-4) were purchased from Sigma Aldrich (Istanbul, Turkey). All materials were analytical grade and used with no further process.

2.2. Sample preparation

Xanthan-based hydrogels were synthesized in the absence or presence of crosslinking agents. The final concentration of Xanthan was fixed at 4 wt.% in all samples. Preparation of samples in the presence of crosslinking agents involved making 1, 2, and 3 wt.% citric acid/borax aqueous solutions followed by adding Xanthan until the total concentration reached 4wt.%. For example, in preparation of Xan-C1 sample (Table 1), 0.1 g citric acid was dissolved in 10 ml deionized water, then 0.4 g Xanthan was added to the system.

The solutions were then mechanically stirred until the gel-like material was obtained. The time of stirring increased with the increased concentration of citric acid and Borax due to the changes in pH. It is worth mentioning that the pH of the aqueous Xanthan solution is neutral and thus the pH of the solutions will be dependent only on the crosslinking agent concentration. Then, the samples were heated to 165 ˚C for 7–10 min to ensure the crosslinks formation (Bueno et al., 2013). The hydrogels were then cast and cooled at room temperature in Petri dishes.

The hydrogels were then dried at 70 ˚C for 48 h to form films. According to (Bueno et al., 2013) these systems are thermally stable at 165 ˚C, and that the crosslinks form while heating at this temperature. Thus, it can be said that no change would occur in the crosslinks during the drying process. The resulted films were kept in a cool dry place until further use. The sample codes, compositions, and the mole content of crosslinkers are given in Table 1

2.3. Rheological measurements

The rheological behavior of the samples was studied by dynamic shear rheometer Physica MCR 301, at parallel plate geometry and 1 mm gap, in frequency sweep mode in the linear viscoelastic region (1% amplitude). The analysis was conducted at 25 ˚C (room temperature) and 37 ˚C (human body temperature) for comparison.

2.4. FTIR analysis

FTIR analysis was conducted to study the crosslinking of the samples using ABB Bomem, MB Series. In this test, the Xan, Xan-C2, and Xan-B2 representative samples were analyzed.

2.5. Polarized optical microscopy

The POM studies were conducted via Olympus BX51 polarized microscope. To study the effect of temperature on the liquid crystalline phase, the samples were exposed to hot airflow of a 100-watt light bulb for 120 min and the imaging was done in defined time intervals.

Table 1
Sample codes and concentrations.

Sample Code	Xanthan wt.%	citric acid wt.%	citric acid mmol	Borax wt.%	Borax mmol
Xan	4	–	–	–	–
Xan–C1	4	1	5.2	–	–
Xan-C2	4	2	10.4	–	–
Xan-C3	4	3	15.6	–	–
Xan-B1	4	–	–	1	2.6
Xan-B2	4	–	–	2	5.2
Xan-B3	4	–	–	3	7.8

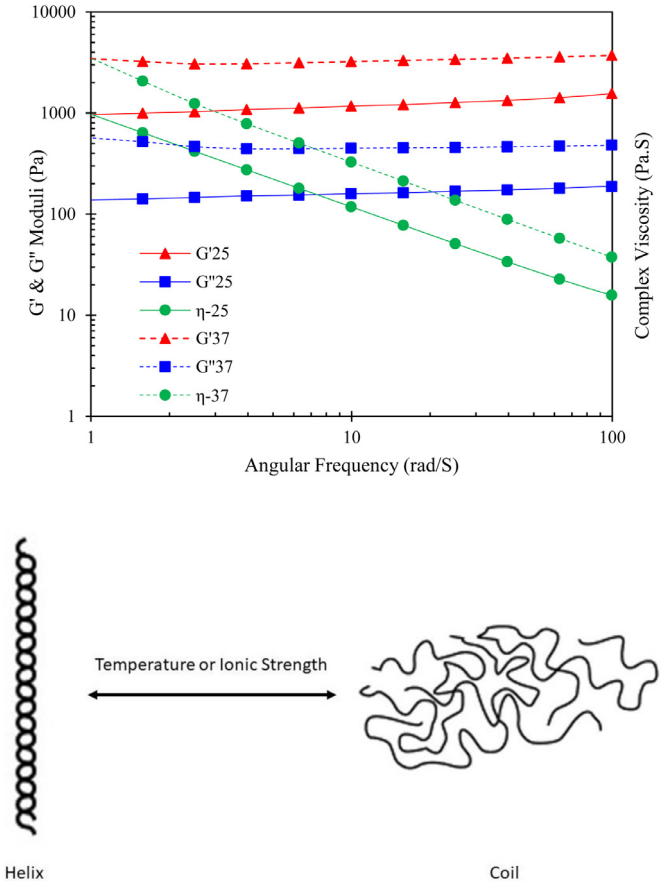


Fig. 1. UP) Rheological behavior of the Xanthan hydrogel at room and body temperatures. DOWN) Schematic illustration of Xanthan order-disorder transition with temperature or ionic strength.

2.6. Scanning electron microscopy

The porosity and surface morphology of the samples were studied using MIRA 3 TE-SCAN scanning electron microscope. The freeze-dried method was considered the best method to observe the pore morphology or inter-polymer network of hydrogels (Yang, Wang, & Kang, 1997). Thus, the samples were freeze-dried at $-80°C$ and then gold sputter-coated prior to SEM analysis.

3. Results and discussion

3.1. Rheological behavior

It has been reported that the rheological behavior of biopolymer solutions are sensitive to changes in temperature, and concentration (Reinoso, Martín-Alfonso, Luckham, & Martínez-Boza, 2019). Fig. 1 – UP shows the rheological behavior of Xanthan hydrogel at room and body temperatures in the absence of cross-linkers. As can be seen, the amounts of storage and loss moduli are almost independent of the angular frequency. The higher amounts of storage modulus (G′) in comparison with loss modulus (G″) is due to the dominant elastic response of the hydrogel because of the high entanglements/interaction of chains. As mentioned before, in our study the concentration of Xanthan is 4 wt.% which is high above the reported C^* of the Xanthan solution and can be considered also higher than the C^{**} concentration reported by some researchers (Oliveira et al., 2013). Therefore, it is expected to observe the solid-like ($G' > G''$) behavior in all frequencies for concentrated Xanthan solutions. Additionally, the decrease in viscosity with increasing frequency can be considered as an indicator of shear thinning behavior in the system.

Rheological analysis in higher temperatures showed the exact same trend pointing out the presence of the gel-like behavior ($G' > G''$) at body temperature as well. However, it is observed that Xanthan hydrogels in the absence of crosslinkers at $37°C$ possess higher amounts of storage modulus and complex viscosity compared to the room temperature. This unexpected observation is due to higher Xanthan chain entanglements at higher temperatures suppressing the movement and fast relaxation of long chains originated from the change in conformation of Xanthan chains from less entangled ordered structure to the more entangled coils. In other words, it can be considered that order-disorder transition is possible to have been occurred in this temperature range in the highly concentrated regime which is not reported before. We have tried to explore the role of crosslinking on this phenomenon in detail throughout different sections.

It is known that Xanthan undergoes a thermally induced conformational change. At lower temperatures, the side chains fold down towards the backbone via non-covalent interactions while at higher temperatures the structure becomes disordered coils and more flexible. The disordered conformation is a result of side chains projecting away from the backbone (Khouryieh, Anton, & Khouryieh, 2006). It has been reported that at 25 °C in distilled water, Xanthan molecules possess a partially ordered conformation. The repulsive interactions between charged side groups expand the chain which could result in a weakly structured material in a semi-dilute regime via hydrogen bonding. Thus, an order-disorder transition could take place with increasing temperature (Khouryieh et al., 2006). The transition could be responsible for the changes in rheological behavior. The order-disorder transition – also known as helix-coil transition - is shown schematically in FIGURE 1 – DOWN which is well accepted in low concentrated regimes (Rochefort & Middleman, 1987). Our results showed that in the concentrated regime, as well, the increase of temperature from 25 to 37 °C resulted in the disordered structure of Xanthan chains and hence a noticeable increase of storage modulus and other rheological properties because of more entanglements in the disordered structure.

It is worth mentioning that although it is widely accepted that the ordered conformation of Xanthan consists of a single helix, Morris (Morris, 2019) discussed that a coaxial double helix is also included. He proposed that both interpretations of ordered Xanthan are correct and that the ordering is a 2-stage process: formation of single helices followed under favorable conditions, by enthalpically-driven conversion to coaxial double helices. The double helix formation causes a doubling of

Table 2
Calculated entanglement density of the Xanthan hydrogels.

Temperature	Average G' (Pa)	Evaluated n ($\frac{mol}{m^3}$)
25°C	1772	0.715
37°C	4486	1.78

molecular weight and mass per unit length (Morris, 2019). The concentration of the biopolymer also affects the conformation of the Xanthan chain and thus, could influence the rheological behavior. It is assumed that low concentration Xanthan solutions demonstrate a disordered conformation while concentrated solutions (around 1wt.%) induce ordered conformation (Reinoso et al., 2019).

Therefore, the increase of the storage modulus and complex viscosity of Xanthan hydrogel during raising the temperature from 25°C to 37°C has been attributed to the reorganization of Xanthan chains and thus increased density of physical entanglements between the macromolecules (Tao et al., 2016). Assuming a Gaussian statistic for the distribution of end-to-end distances, the theory of rubber elasticity (Eqn. 1) could be used to quantify the entanglements density as shown in Table 2.

$$G' = nRT \tag{1}$$

It is observed that the entanglements density, n, at $37°C$ is almost 2.5 times the value of n at $25°C$. As mentioned earlier, this research hypothesizes that the order-disorder transition can occur between $25°C - 37°C$ in a concentrated Xanthan solution. The observed increase in crosslinking density value strengthens this hypothesis. The higher crosslinking density could be attributed to the coiled conformation in which physical entanglements are present.

Fig. 2 shows the rheological behavior of Xanthan hydrogels in the presence or absence of the 2 wt.% bi-functional and tetra-functional crosslinking agents. It is noticeable that the molar amount of citric acid in the 2 wt.% sample is 150 mmol, while it is 52 mmol for Borax in the relative sample as mentioned in Table 1.

The same rheological characteristics, i.e. solid like in the whole frequency range and shear thinning behavior are seen for all hydrogels. The G'' curves are not shown in Fig. 2 for simplification. The shear-thinning behavior, which is indicated by the decrease of complex viscosity amounts with increasing angular frequency, can be seen in Fig. 2-b.

Fig. 2 also compares the effect of Borax and citric acid as crosslinking agents for hydrogels with 2wt.% cross-linker. The values for other concentrations can be found in other graphs and thus there is no need to be replicated here. It is shown that at room temperature almost no change in the amount of storage modulus has been observed for the neat Xanthan hydrogel and crosslinked hydrogels. This can be due to the dominant pseudo-gel nature of concentrated hydrogels and the ordered structure of Xanthan chains at room temperature. In other words, at room temperature crosslinking cannot change the conformation and mobility of the chains therefore no changes in storage modulus and complex viscosity were observed.

Interestingly, the difference between samples is pronounced at elevated temperatures. At 37 °C crosslinked hydrogels demonstrate a decrease in the G' amounts as shown in Fig. 2-a.

Some reasons can be considered for this behavior. The first reason that could be considered is the effect of the crosslinks on the prevention of the chain movement at higher temperatures. As has been mentioned earlier, the physical entanglements in the disordered conformation are responsible for the higher storage modulus. Here, the presence of the crosslinks seems to prevent the transformation of the ordered helix to disordered coil conformation. Consequently, the physical entanglements in the disordered conformation are not able to recover; therefore, the storage modulus cannot increase in crosslinked hydrogel so far.

Second, electrostatic charges of the Xanthan chain at alkaline and acidic pH can be considered as one of the main reasons which are more effective at the higher temperature (García-Ochoa et al., 2000; Rwei & Nguyen, 2014). In other words, at higher temperature electrostatic repulsion may result in decreasing the physical entanglement and hence suppressing the storage modulus.

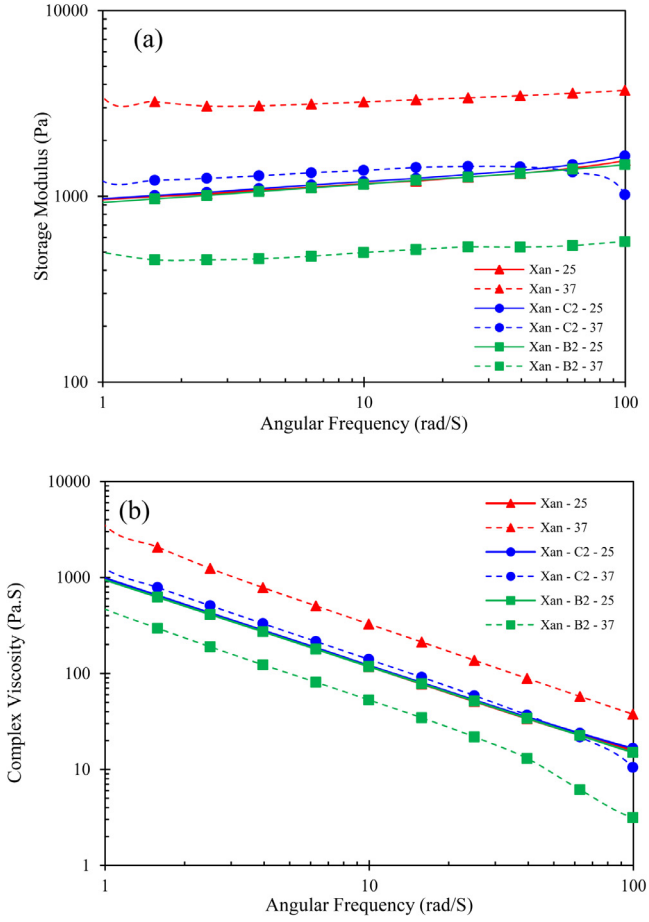


Fig. 2. Rheological behavior of Xanthan hydrogels, a) Storage Modulus amounts, and b) Complex Viscosity amounts.

Considering the decrease of the rheological properties in the Xan-B2 below the value for non-crosslinked Xanthan hydrogels, one can assume both reasons are involved in rheological behavior. In this regard, the decrease of the storage modulus and complex viscosity of Xan-B2 is attributed to the prevention of the conformational change of the ordered Xanthan helixes to disordered chains because of Borax crosslinks as well as changing the pH of the system. Also, the decrease in storage modulus for Xan-B2 sample is higher compared to Xan-C2 sample, which is the result of stronger movement prevention effect of Borax cross-links which could be attributed to tetra-directional crosslinks in this system. From another point of view, it can be inferred that the effect of alkaline conditions on conformational changes of Xanthan chains at higher temperatures is stronger than acidic conditions (Bejenariu et al., 2009; Bejenariu et al., 2010). Therefore, the nature of the crosslinkers may affect rheological behaviors differently. It is worth mentioning that the concentration of the functional groups of Borax and citric acid is almost identical in the samples. For example, in the Xan-C2 sample, the concentration of active sites is almost 20.8 mmol – considering two active sites for each molecule. This is also the case for Xan-B2 sample in which the concentration of the active sites is almost 20.8 mmol – considering four active sites for each molecule. In other words, although the amount of functional group of two crosslinker is the same, more functional groups are involved in crosslinking reaction in Borax containing samples which is attributed to the more alkaline conditions, leading to the higher crosslinking density.

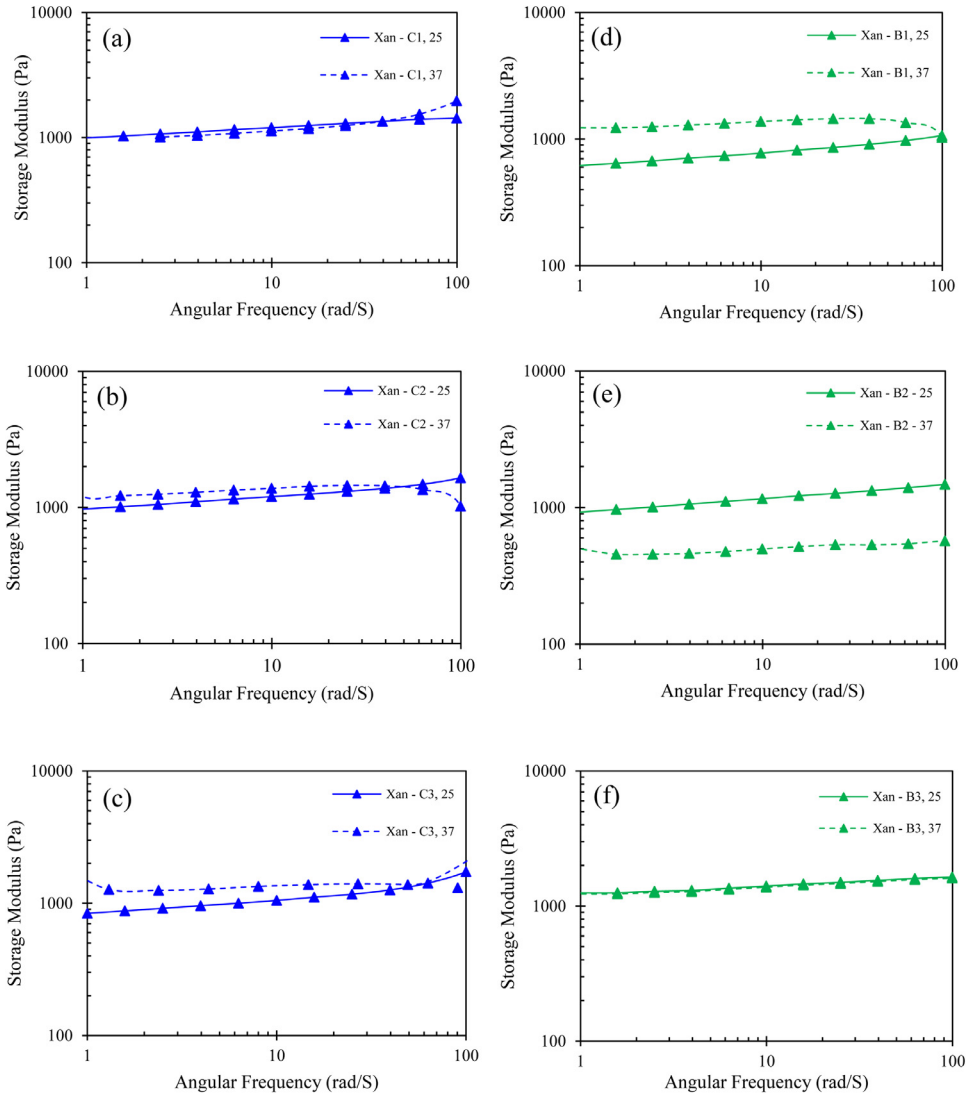


Fig. 3. Effect of temperature on the storage modulus of Xanthan hydrogels with a) 1wt.%, b) 2wt.% and c) 3wt.% of citric acid and d) 1wt.% e) 2wt.% and f) 3wt.% of Borax.

Fig. 3 shows the effect of temperature on the storage modulus of Xanthan hydrogel crosslinked with different concentrations of citric acid and Borax. As can be seen in Fig. 3-a–c, the storage modulus of citric acid crosslinked hydrogels is almost independent of temperature in all concentrations. However, at the lower concentration, as shown in Fig. 3-a, the storage modulus is slightly decreased at 37 ˚C compared to that of the 25 ˚C. This can be explained by the fact that the presence of citric acid as a crosslinking agent, limits the reorganization of Xanthan chains, and thus, the storage modulus cannot change drastically.

Additionally, although the increase in the concentration of citric acid should enhance the crosslinks density and prevent the disorder transition, the change in pH toward the lower values might favor the disorder transition of Xanthan chains and hence increase the physical entanglements. Thus, these two opposite effects may compensate each other resulting in a little change in the storage modulus of the citric acid crosslinked hydrogel. It should be mentioned here that the storage modulus of the un-crosslinked hydrogel at 37 ˚C, (3220 Pa at 996 rad/s) is much higher than that of the crosslinked samples (e.g. 1380 Pa at 996 rad/s for Xan-C2 sample) due to its disorder conformation and physical entanglements.

Fig. 3 also shows the effect of temperature and crosslinking agent concentration on Xanthan – Borax hydrogels. The graphs are similar to those of Xanthan – citric acid indicating similar behavior, but it seems that Xanthan chains are more strongly influenced by Borax. This could be due to a known fact that a weak alkaline media forms due to hydrolysis of Borax which could further influence the G' amounts of a hydrogel. It is observed that the amount of storage modulus for Xanthan hydrogel crosslinked with 1 wt.% Borax does not change significantly with temperature from 25 ˚C to 37 ˚C.

For hydrogels with 2 wt.% of Borax, a decrease in G' amount has been observed at 37 ˚C, which might have happened due to the dominant effect of Borax crosslinks on the prevention of order-disorder transition of Xanthan helixes as it was mentioned earlier. This effect has been compromised at higher Borax concentration. This could be due to higher rates of hydrolysis at 37 ˚C, causing a reduction in the density of crosslinks which allows the chains to get more entangled; hence increasing the storage modulus as shown in Fig. 3-f. These results indicate the effect of crosslinker type on the rheological behavior of concentrated Xanthan hydrogels. In the systems with Borax as a crosslinker, the rheological behavior is more sensitive to concentration and temperature than the citric acid crosslinked hydrogels.

3.2. *Crosslinking mechanism*

Reddy et. Al. suggested a mechanism for crosslinking of Xanthan via citric acid during which, a condensation process occurs at 165 ˚C with dehydration and ester linkages formation (Yang et al., 1997; Reddy & Yang, 2010). Generally, these kinds of bonding create three-

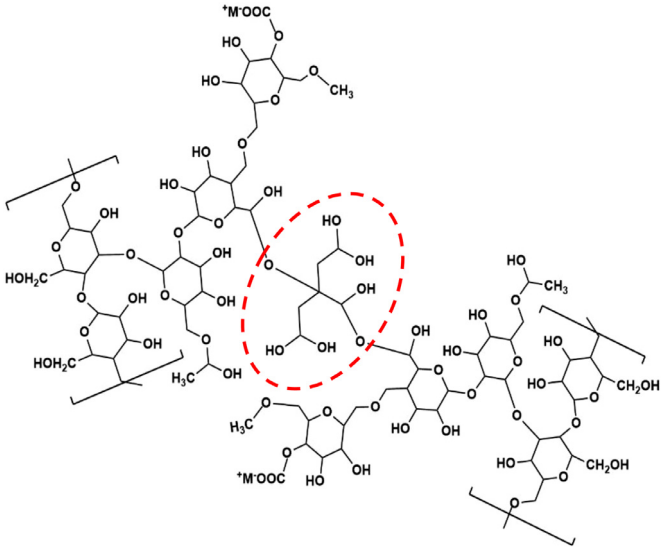
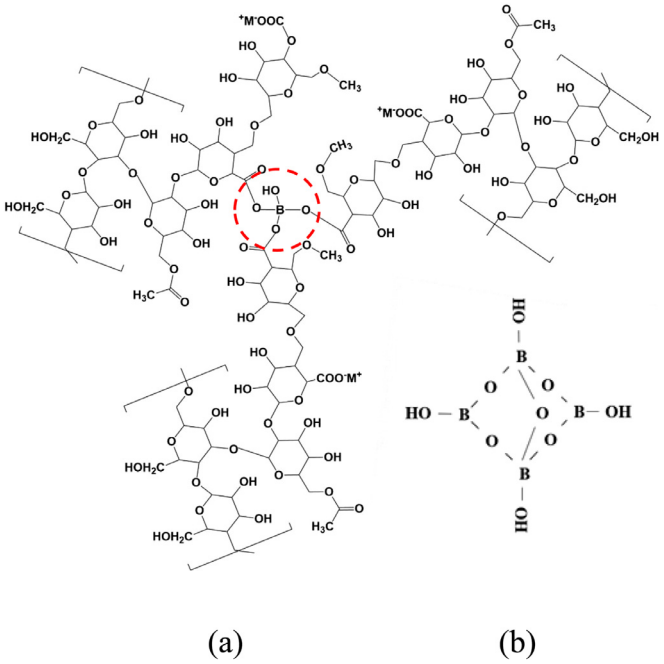


Fig. 4. Schematic illustration of crosslinking Xanthan with citric acid.



(a) (b)

Fig. 5. a) Suggested mechanism for Xanthan crosslinking via Borax. For simplification, the middle part of the Borax molecule has been denoted as "B". b) Borax structure schematic

dimensional hydrophilic structures known as chemical hydrogels. Bueno et al. (Bueno et al., 2013) used thermogravimetric analysis to show that xanthan chains are stable at this temperature. This mechanism has been illustrated in Fig. 4 (Bueno et al., 2013; Yang et al., 1997). It is worth mentioning that in the absence of any crosslinking agent, esterification between hydroxyl groups and pyruvyl/acetyl groups of the xanthan chains can occur upon heating (Bueno et al., 2013), resulting in hydrogel formation in native samples. This mechanism has been the basis of our hypothesis on crosslinking Xanthan via Borax, as will be discussed later.

As discussed in the previous section, the preventing effect of Borax is stronger than citric acid. These observations have been attributed to the higher crosslinking density in the Xanthan-Borax system and lead to an assumption that a higher density of crosslinking is due to more active sites on Borax molecule (Fig. 5b) participated in reaction with Xanthan chains. This assumption has schematically shown in Fig. 5 and further studied with FTIR analysis in the next section. For simplification, the middle part of the Borax molecule in Fig. 5a has been denoted as "B" in the schematic mechanism.

It is supposed that the same reactions occur in crosslinking Xanthan with Borax to that of citric acid, as the involved groups are similar. Thus, it is expected that an esterification reaction happens in Xanthan – Borax system by heating. Although the reactions seem to be similar, the main difference between the two systems is the number of active sites getting involved to form ester linkages. Due to steric restrictions, only two hydroxyl groups of citric acid can be involved in the crosslinking process as opposed to Borax. It is expected that at least three hydroxyl groups of Borax molecule engage in the linkages.

Fig. 6 demonstrate the FTIR analysis of the samples. For Xanthan – citric acid hydrogels, the 801 and 894 cm^{-1} peaks are thought to appear because of the formation of C-O-C bonds due to the formation of crosslinks. Also, in FTIR analysis of the Xanthan – Borax the 2263 and 2367 cm^{-1} peaks represent the B-O-C bonds formed during crosslinking. It is known that Xanthan has a characteristic peak at 1735 cm^{-1} due to C=O stretch of COO^{-1} in pyruvate and glucuronate groups (Lal, Dubey, Gaur, Verma, & Verma, 2017). FIGURE 6 shows a peak in 1728 cm^{-1} which is thought to be the characteristic peak of Xanthan. Quantitative analysis of the FTIR data was done by normalizing the intensities to the reference peak (1728 cm^{-1}) and calculating the area under the characteristic peak of each sample. The area under reference peak for Xanthan, Xanthan – B2, and Xanthan – C2 samples are calculated as 49.79, 79.83, and 148.5, respectively. Also, the area under the characteristic peak for

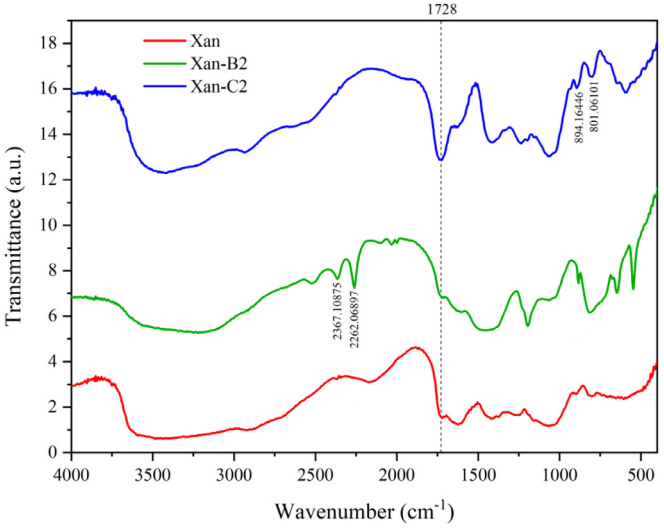


Fig. 6. FTIR analysis of the samples.

Xanhan – B2 and Xanthan – C2 are 324.78 and 182.77, respectively. It can be concluded that the area under the Xan-B2 graph in the 2500 – 2000 cm^{-1} interval -which is related to B-O-C bands- is bigger than Xan-C2 graph. This is contributed to the higher density of B-O-C bands which proves the fact that more active sites on Borax molecule lead to higher crosslinking densities.

The different effects of bifunctional and tetra-functional crosslinkers have been schematically illustrated in Fig. 7.

3.3. Polarized optical microscopy (POM)

The LC-isotropic phase transition is affected by temperature as well. It has been investigated that a slow phase transition occurs in high temperatures. Fig. 8 demonstrates the POM images of hydrogel samples exposed to hot airflow. It can be seen that the longer samples exposed to

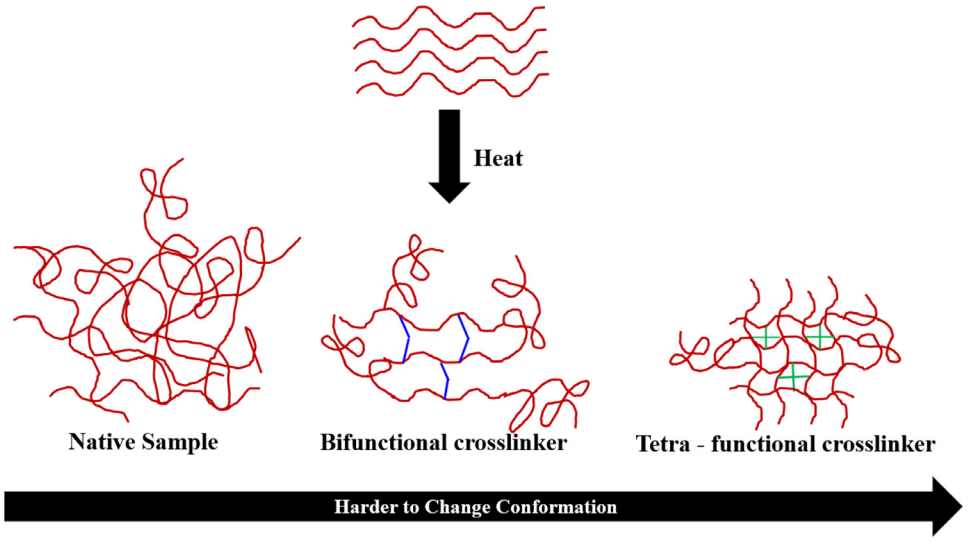


Fig. 7. Schematic representation of different types of crosslinkers (bi/tetra-functional) effect on the reorganization of Xanthan chains.

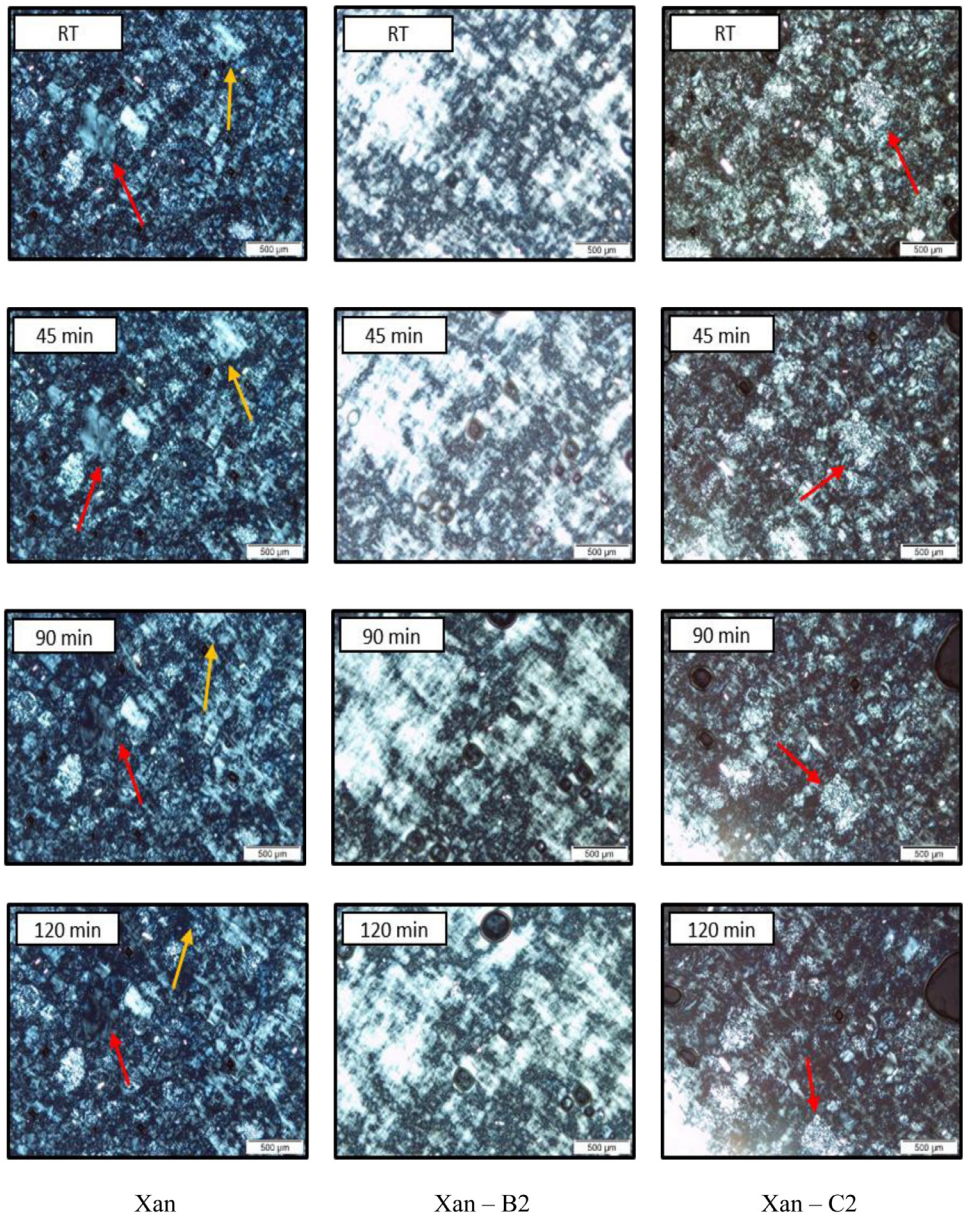


Fig. 8. POM images of Xan, Xan – B2, and Xan – C2 samples after being exposed to hot air flow for defined time intervals.

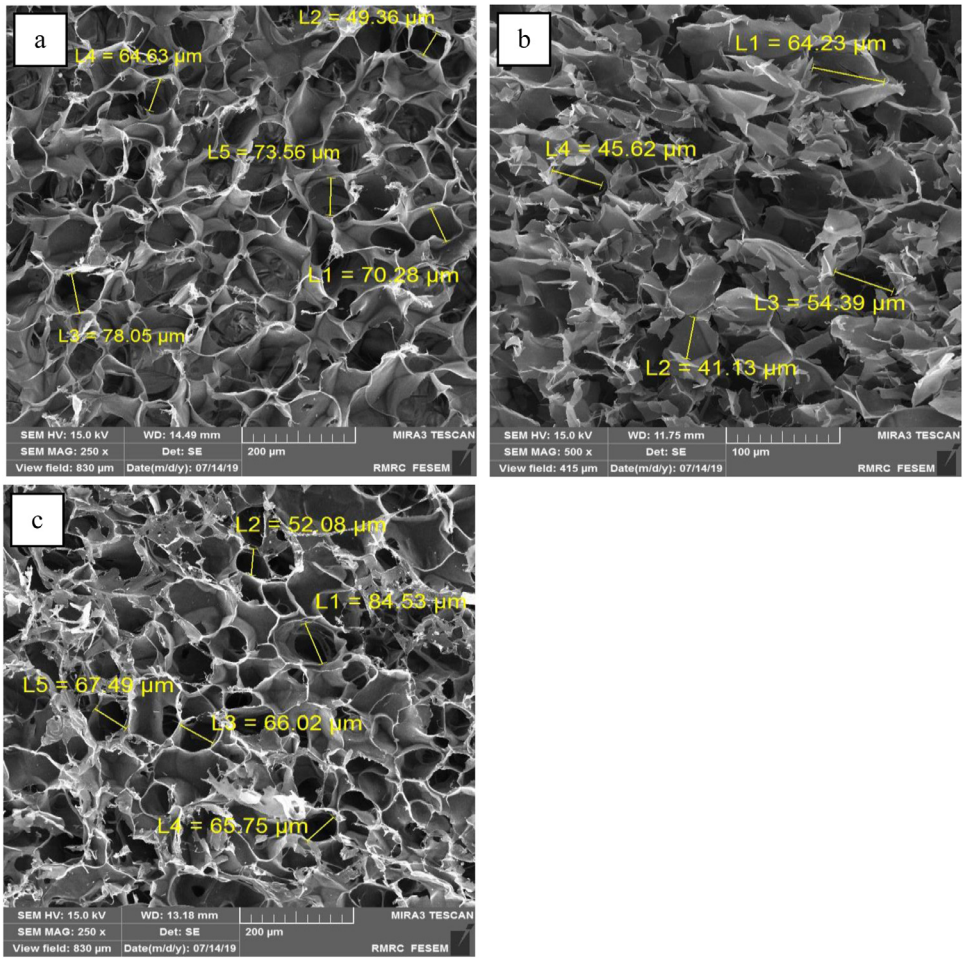


Fig. 9. SEM images of the surface morphology of samples a) Xan, b) Xan – B2, and c) Xan – C2.

hot airflow, the more shrinkage occurs in the liquid crystalline phase. This phenomenon was expected since increasing temperature causes the hydrogen bonds to start breaking up and thus the ordered morphology of the liquid crystalline phase falls apart.

It had been supposed that using Borax and citric acid as crosslinking agents, prevents the conformational change of the Xanthan molecules and the effect of Borax is stronger than citric acid, owing to more active sites on Borax molecule. The polarized optical microscopy images demonstrated the same trend. As it can be seen in Fig. 8, heating native Xanthan samples for 120 minutes changes the texture of the images in an obvious manner. However, there is a delay in observing texture alteration in crosslinked samples in comparison to non-crosslinked samples. This is attributed to the fact that Xanthan molecules need more relaxation time when they are crosslinked. The POM images reveal that the texture change in Xan – C2 sample could be observed after 90 min of being exposed to hot air flow whilst no significant change is observed in Xan – B2 sample after 120 minutes.

Additionally, it is seen that at room temperature (RT) the area of the LC phase (brighter region) in Xan – B2 sample is higher than Xan – C2 sample, which is in turn, bigger than Xan sample. This is attributed to higher crosslinking density in the presence of Borax which causes more Xanthan molecules to form rod-like conformation which is the characteristic of a liquid crystalline phase.

The results also illustrate that the change in the texture for Xan – B2 and Xan – C2 samples occur slower than native Xanthan, attributing to the prevention effect of crosslinks. In other words, crosslinks presence limits the chain mobility of the Xanthan molecules and thus enhancing the required time for the LC phase to disrupt, which happens in response to the elimination of the ordered conformation of Xanthan molecules. Conclusively, the POM images showed the liquid crystalline characteristics of the concentrated samples and the difference between two crosslinker agents, qualitatively. However, although these results are in line with rheological measuring the more accurate experiment using a hot stage microscope is necessary for an in-depth and quantitative study of the liquid crystalline nature of concentrated Xanthan-based hydrogel sample which was out of the scope of our study.

3.4. SEM analysis

The morphological study was done by scanning electron microscopy (Fig. 9) and the images were analyzed by ImageJ. It is known that the hydrogels with denser and tighter structure have smaller pore sizes (Yacob & Hashim, 2014). The pore sizes were measured as $64.71 \pm 14.012\ \mu m$ for Xanthan, $62.47 \pm 13.179\ \mu m$ for Xanthan – citric acid, and $57.96 \pm 16.553\ \mu m$ for Xanthan – Borax samples. It is known that higher crosslinking density causes shortening in the inter-chains distance which could result in smaller pore sizes (Satani, Kuwata, & Shimizu, 2020). It is observed that the difference in the average pore size for native Xanthan and Xanthan – citric acid samples is not as high as Xanthan – Borax sample. This shows that the physical entanglements which form in highly concentrated Xanthan solutions can influence the porosity of the hydrogels almost the same as chemical crosslinks formed in the presence of citric acid. However, the Borax - crosslinked sample shows smaller pore sizes which could be attributed to higher crosslinking density. It should be noted that high standard deviation values are due to inhomogeneity of the pore shapes which make the measurements quite hard.

4. Conclusion

It is known that the Xanthan chains go through a conformational change in high temperatures. According to the rheological study, Xanthan hydrogels possess an increase in the storage and loss modulus with increasing temperature. This behavior has been attributed to the prevention of conformational change due to chain entanglements and crosslinks. The effect of crosslinker concentration was also investigated and showed that changes in the concentration of Borax has stronger effects on rheological behavior compared to citric acid. It is concluded that the prevention effect of Borax on Xanthan chains is stronger compared to citric acid. FTIR analysis has proved the hypothesis that the higher influence of Borax on Xanthan chains is due to higher degrees of crosslinking which is formed on more active sites on Borax molecule. Also, rheological behavior and FTIR results were analyzed to suggest a mechanism for the crosslinking of Xanthan by Borax. Polarized Optical Microscopy was done to illustrate the liquid crystalline phase formed in Xanthan solutions. The texture change trend of the samples was compatible with the previous data, confirming the stronger effect of Borax to prevent the conformation change of the Xanthan molecules. Also, SEM images were used to study the surface morphology and porosities of the hydrogels. These results provide some valuable and fundamental information for the development of the concentrated xanthan-based hydrogels with tunable gel strength and temperature-dependent properties for further use in biomaterials, biomedical, and food engineering applications. For example, concentrated crosslinked Xanthan hydrogels can be considered for smart wound dressing materials with controlled rheological properties and drug release rate.

Declaration of Competing Interest

The authors declare that they have no known competing financial interests or personal relationships that could have appeared to influence the work reported in this paper.

References

Ahmed, E. M. (2015). Hydrogel: Preparation, characterization, and applications: A review. *Journal of Advanced Research, 6*(2), 105–121. https://doi.org/10.1016/j.jare.2013.07.006.

Allain, C., Lecourtier, J., & Chauveteau, G. (1988). Mesophase formation in high molecular-weight xanthan solutions. *Rheologica Acta, 27*, 255–262.

Alupei, I. C., Popa, M., Hamcerencu, M., & Abadie, M. J. M (2002a). Superabsorbant hydrogels based on xanthan and poly(vinyl alcohol): 1. The study of the swelling properties. *European Polymer Journal, 38*(11), 2313–2320. https://doi.org/10.1016/S0014-3057(02)00106-4.

Alupei, I. C., Popa, M., Hamcerencu, M., & Abadie, M. J. M (2002b). Superabsorbant hydrogels based on xanthan and poly(vinyl alcohol). *European Polymer Journal, 38*(11), 2313–2320. https://doi.org/10.1016/S0014-3057(02)00106-4.

Annabi, N., Tamayol, A., Uquillas, J. A., Akbari, M., Bertassoni, L. E., Cha, C., … Khademhosseini, A. (2014). 25th anniversary article: Rational design and applications of hydrogels in regenerative medicine. *Advanced Materials, 26*(1), 85–124. https://doi.org/10.1002/adma.201303233.

Bejenariu, A., Popa, M., Dulong, V., Picton, L., & Le Cerf, D. (2009). Trisodium trimetaphosphate crosslinked xanthan networks: Synthesis, swelling, loading and releasing behaviour. *Polymer Bulletin, 62*(4), 525–538. https://doi.org/10.1007/s00289-008-0033-8.

Bejenariu, A., Popa, M., Picton, L., & Le Cerf, D. (2010). Effect of concentration, pH and temperature on xanthan conformation: A preliminary study before crosslinking. *Revue Roumaine de Chimie, 55*(2), 147–152.

Boyd, M. J., Hampson, F. C., Jolliffe, I. G., Dettmar, P. W., Mitchell, J. R., & Melia, C. D. (2009). Strand-like phase separation in mixtures of xanthan gum with anionic polyelectrolytes. *Food Hydrocolloids, 23*(8), 2458–2467. https://doi.org/10.1016/J.FOODHYD.2009.07.008.

Brunchi, C. E., Avadanei, M., Bercea, M., & Morariu, S. (2019). Chain conformation of xanthan in solution as influenced by temperature and salt addition. *Journal of Molecular Liquids, 287*, Article 111008. https://doi.org/10.1016/j.molliq.2019.111008.

Bueno, V. B., Bentini, R., Catalani, L. H., & Petri, D. F. S (2013). Synthesis and swelling behavior of xanthan-based hydrogels. *Carbohydrate Polymers, 92*(2), 1091–1099. https://doi.org/10.1016/j.carbpol.2012.10.062.

Burchard, W. (2001). Structure formation by polysaccharides in concentrated solution. *Biomacromolecules, 2*, 342–353. https://doi.org/10.1021/bm0001291.

Caló, E., & Khutoryanskiy, V. V. (2015). Biomedical applications of hydrogels: A review of patents and commercial products. *European Polymer Journal, 65*, 252–267. https://doi.org/10.1016/J.EURPOLYMJ.2014.11.024.

Cuvelier, G., & Launay, B. (1986). Concentration regimes in xanthan gum solutions deduced from flow and viscoelastic properties. *Carbohydrate Polymers, 6*(5), 321–333. https://doi.org/10.1016/0144-8617(86)90023-8.

Dixit, A., Bag, D. S., Sharma, D. K., & Eswara Prasad, N. (2019). Synthesis of multifunctional high strength, highly swellable, stretchable and self-healable pH-responsive ionic double network hydrogels. *Polymer International, 68*(3), 503–515. https://doi.org/10.1002/pi.5741.

Dong, Y., Mao, W., Wang, H., Zhao, Y., Li, X., Bi, D., … Fang, X. (2006). Measurement of critical concentration for mesophase formation of chitosan derivatives in both aqueous and organic solutions. *Polymer International, 55*, 1444–1449. https://doi.org/10.1002/pi.2099.

Edens, R. E. (2005). Polysaccharides: Structural diversity and functional versatility. *Journal of the American Chemical Society, 127*(28), 10119. https://doi.org/10.1021/ja0410486.

García-Ochoa, F., Santos, V., Casas, J., & Gómez, E. (2000). Xanthan gum: production, recovery, and properties. *Biotechnology Advances, 18*(7), 549–579. https://doi.org/10.1016/S0734-9750(00)00050-1.

Hamcerencu, M., Popa, M., Riess, G., & Desbrieres, J. (2019). Chemically modified xanthan and gellan for preparation of biomaterials for ophthalmic applications. *Polymer International*, (October). https://doi.org/10.1002/pi.5927.

Iseki, T., Takahashi, M., Hattori, H., Hatakeyama, T., & Hatakeyama, H. (2001). Viscoelastic properties of xanthan gum hydrogels annealed in the sol state. *Food Hydrocolloids, 15*(4–6), 503–506. https://doi.org/10.1016/S0268-005X(01)00088-1.

Khouryieh, H., Anton, H., & Khouryieh, M. (2006). *Rheological characterization of Xanthan-Guar mixtures in dilute solutions*. Kansas State University.

Kopeček, J., & Yang, J. (2007). Hydrogels as smart biomaterials. *Polymer International, 56*(9), 1078–1098. https://doi.org/10.1002/pi.2253.

Lal, N., Dubey, J., Gaur, P., Verma, N., & Verma, A. (2017). Chitosan based in situ forming polyelectrolyte complexes: A potential sustained drug delivery polymeric carrier for high dose drugs. *Materials Science and Engineering C, 79*(May), 491–498. https://doi.org/10.1016/j.msec.2017.05.051.

Li, H., Rief, M., Oesterhelt, F., & Gaub, H. E. (1999). Force spectroscopy on single xanthan molecules. *Applied Physics A, 68*(4), 407–410. https://doi.org/10.1007/s003390050914.

Maret, G., Milas, M., & Rinaudo, M. (1981). Cholesteric order in aqueous solutions of the polysaccharide Xanthan. *Polymer Bulletin, 4*(5), 291–297. https://doi.org/10.1007/BF00255106.

Milas, M. (1990). Structure and properties of xanthan versus fermentation time in an emulsion system. *Carbohydrate Polymers, 13*(2), 119–131. https://doi.org/10.1016/0144-8617(90)90079-8.

Milas, M, Rinaudo, M., & Tinland, B. (1985). The viscosity dependence on concentration, molecular weight and shear rate of xanthan solutions. *Polymer Bulletin, 14*(2), 157–164. https://doi.org/10.1007/BF00708475.

Milas, Michel, & Rinaudo, M. (1979). Conformational investigation on the bacterial polysaccharide xanthan. *Carbohydrate Research, 76*(1), 189–196. https://doi.org/10.1016/0008-6215(79)80017-8.

Morris, E. R. (2019). Ordered conformation of xanthan in solutions and "weak gels": Single helix, double helix – or both? *Food Hydrocolloids, 67*(June 2017), 18–25. https://doi.org/10.1016/j.foodhyd.2017.11.036.

Oliveira, P. D., Michel, R. C., McBride, A. J. A., Moreira, A. S., Lomba, R. F. T., & Vendruscolo, C. T (2013). Concentration regimes of biopolymers Xanthan, Tara, and Clairana, comparing dynamic light scattering and distribution of relaxation time. *PLoS One, 8*(5), 2–8. https://doi.org/10.1371/journal.pone.0062713.

Ortiz-Tafoya, M. C., Rolland-Sabaté, A., Garnier, C., Valadez-García, J., & Tecante, A. (2018). Thermal, conformational and rheological properties of κ-carrageenan-sodium stearoyl lactylate gels and solutions. *Carbohydrate Polymers, 193*(January), 289–297. https://doi.org/10.1016/j.carbpol.2018.04.002.

Pelletier, E., Viebke, C., Meadows, J., & Williams, P. A. (2001). A rheological study of the order–disorder conformational transition of xanthan gum. *Biopolymers, 59*(5), 339–346. https://doi.org/10.1002/1097-0282(20011015)59:5⟨339::aid-bip1031⟩3.3.co;2-1.

Reddy, N., & Yang, Y. (2010). Citric acid cross-linking of starch films. *Food Chemistry, 118*(3), 702–711. https://doi.org/10.1016/J.FOODCHEM.2009.05.050.

Reinoso, D., Martín-Alfonso, M. J., Luckham, P. F., & Martínez-Boza, F. J. (2019). Rheological characterisation of xanthan gum in brine solutions at high temperature. *Carbohydrate Polymers*, (June 2018), 103–109. https://doi.org/10.1016/j.carbpol.2018.09.034.

Rochefort, W. E., & Middleman, S. (1987). Rheology of Xanthan Gum: Salt, Temperature, and Strain Effects in Oscillatory and Steady Shear Experiments. *Journal of Rheology, 31*(4), 337–369. https://doi.org/10.1122/1.549953.

Rodd, A. B., Dunstan, D. E., & Boger, D. V. (2000). Characterisation of xanthan gum solutions using dynamic light scattering and rheology. *Carbohydrate Polymers, 42*(2), 159–174. https://doi.org/10.1016/S0144-8617(99)00156-3.

Rwei, S. P., & Nguyen, T. A. (2014). Phase formation and transition in a xanthan gum/H2O/H3PO4 tertiary system. *Cellulose, 21*(3), 1277–1288. https://doi.org/10.1007/s10570-014-0193-7.

Satani, H., Kuwata, M., & Shimizu, A. (2020). Simple and environmentally friendly preparation of cellulose hydrogels using an ionic liquid. *Carbohydrate Research, 494*(February), Article 108054. https://doi.org/10.1016/j.carres.2020.108054.

Sereno, N. M., Hill, S. E., & Mitchell, J. R. (2007). Impact of the extrusion process on xanthan gum behaviour. *Carbohydrate Research, 342*(10), 1333–1342. https://doi.org/10.1016/j.carres.2007.03.023.

Southwick, J. G., Lee, H., Jamieson, A. M., & Blackwell, J. (1980). Self-association of xanthan in aqueous solvent-systems. *Carbohydrate Research, 84*(2), 287–295. https://doi.org/10.1016/S0008-6215(00)85558-5.

Tao, Y., Zhang, R., Xu, W., Bai, Z., Zhou, Y., Zhao, S., … Yu, D. (2016). Rheological behavior and microstructure of release-controlled hydrogels based on xanthan gum crosslinked with sodium trimetaphosphate. *Food Hydrocolloids, 52*, 923–933. https://doi.org/10.1016/J.FOODHYD.2015.09.006.

Yacob, N., & Hashim, K. (2014). Morphological effect on swelling behaviour of hydrogel. *AIP Conference Proceedings, 153*(February), 153–159. https://doi.org/10.1063/1.4866123.

Yang, C. Q., Wang, X., & Kang, I.-S. (1997). Ester Crosslinking of Cotton Fabric by Polymeric Carboxylic Acids and Citric Acid. *Textile Research Journal, 67*(5), 334–342. https://doi.org/10.1177/004051759706700505.

Yoshida, H., Hatakeyama, T., & Hatakeyama, H. (1990). Phase transitions of the water-xanthan system. *Polymer, 31*(4), 693–698. https://doi.org/10.1016/0032-3861(90)90291-6.

Zuev, V. V, Kostromin, S. V, & Bronnikov, S. V. (2008). Nature of the liquid-crystalline phase in supramolecular linear polymers. *Polymer Science Series B, 50*(7), 177–181. https://doi.org/10.1134/S1560090408070051.